TECHNICAL REPORT M-71-6

PREDICTION OF THE SLOPE-CLIMBING CAPABILITY OF ELASTIC-RIM WHEELS

by

K. W. Wiendieck

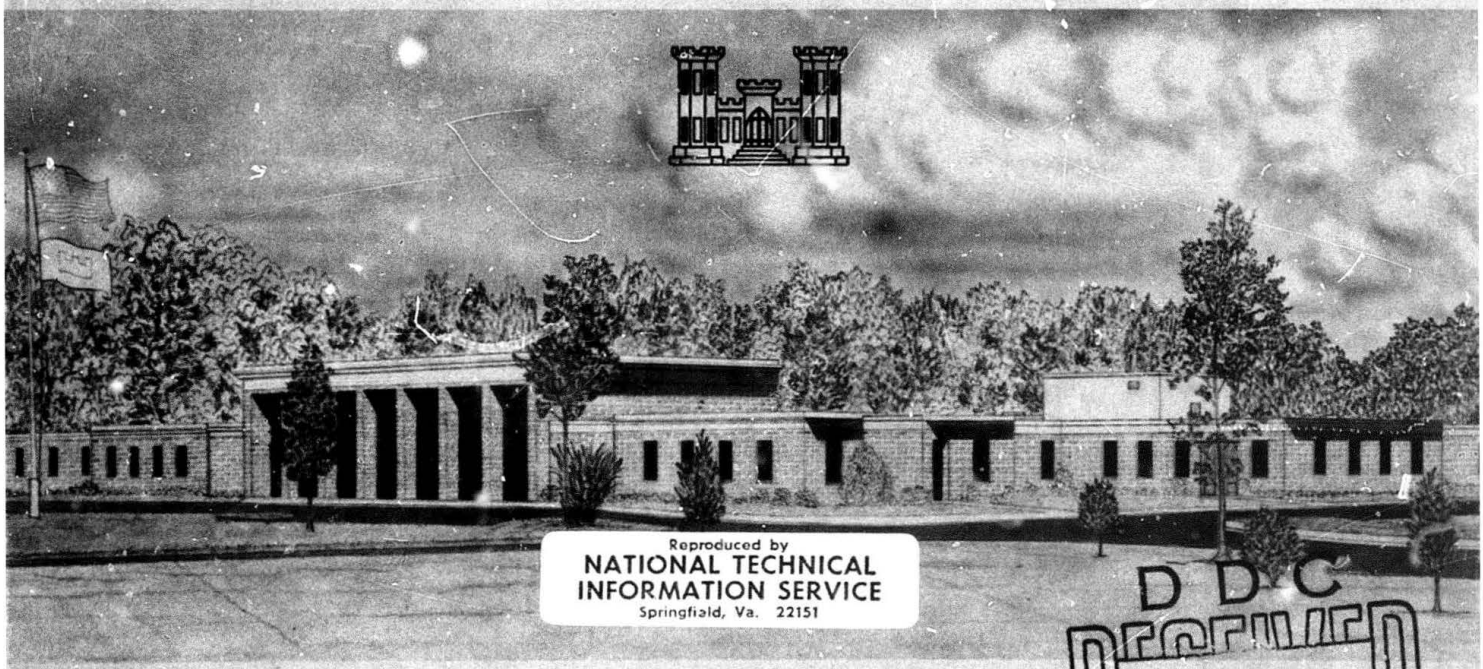

September 1971

Sponsored by U. S. Army Materiel Command

Conducted by U. S. Army Engineer Waterways Experiment Station, Vicksburg, Mississippi

Destroy this report when no longer needed. Do not return it to the originator.

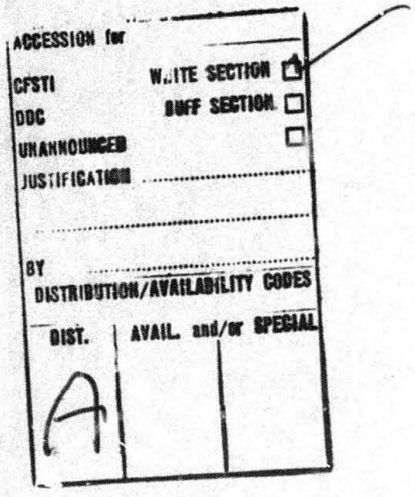

The findings in this report are not to be construed as an official Department of the Army position unless so designated by other authorized documents.

TECHNICAL REPORT M-71-6

PREDICTION OF THE SLOPE-CLIMBING CAPABILITY OF ELASTIC-RIM WHEELS

by

K. W. Wiendieck

September 1971

Sponsored by U. S. Army Materiel Command
Project 1T061102B52A, Task 01

Conducted by U. S. Army Engineer Waterways Experiment Station, Vicksburg, Mississippi

ARMY-MRC VICKSBURG, MISS.

Unclassified

Security Classification

DOCUMENT CONTROL DATA - R & D

(Security classification of title, body of abstract and indexing annotation must be entered when the overall report is classified)

1. ORIGINATING ACTIVITY (Corporate author) U. S. Army Engineer Waterways Experiment Station Vicksburg, Mississippi	2a. REPORT SECURITY CLASSIFICATION Unclassified 2b. GROUP

3. REPORT TITLE

PREDICTION OF THE SLOPE-CLIMBING CAPABILITY OF ELASTIC-RIM WHEELS

4. DESCRIPTIVE NOTES (Type of report and inclusive dates)

Final report

5. AUTHOR(S) (First name, middle initial, last name)

Klaus W. Wiendieck

6. REPORT DATE	7a. TOTAL NO. OF PAGES	7b. NO. OF REFS
September 1971	50	8

8a. CONTRACT OR GRANT NO.	9a. ORIGINATOR'S REPORT NUMBER(S)
b. PROJECT NO. 1T061102B52A, Task 01	Technical Report M-71-6
c.	9b. OTHER REPORT NO(S) (Any other numbers that may be assigned this report)
d.	

10. DISTRIBUTION STATEMENT

Approved for public release; distribution unlimited.

11. SUPPLEMENTARY NOTES	12. SPONSORING MILITARY ACTIVITY
	U. S. Army Materiel Command Washington, D. C.

13. ABSTRACT A new semiempirical approach was attempted to predict the slope-climbing capability of wheels. This approach consisted of determining the pull performance of flexible wheels on yielding slopes by two extrapolations: one starting from the theoretically known pull performance of flexible wheels on unyielding slopes, and the other from experimentally determined performance of rigid wheels on yielding, level ground. The result is a prediction equation for the available pull of elastic-rim wheels (as a particularly simple case of pneumatic tires) on deformable, inclined soils in terms of soil deformability, cohesion, and internal friction; wheel flexibility and load; and slope angle. Various reduction factors developed to take sinkage and load effects into account were adjusted to satisfy known conditions and to make the two extrapolations compatible. By solving the prediction equation for zero pull, maximum slope-climbing capability can be determined; and by solving for zero slope, the maximum pull/load ratio on level ground can be obtained. Although the equation lacks theoretical rigor, it matches the extreme conditions on both ends of the soil and wheel deformability spectra and is thought to describe intermediate conditions with a high degree of confidence. The equation has been checked numerically only for the test conditions provided by elastic-rim wheels (Bendix lunar wheels) because they exhibited the simple deformation characteristics that were needed for this first formulation of a new approach. The more complex behavior of tires can be included in an extension of the study.

DD FORM 1 NOV 68 1473 REPLACES DD FORM 1473, 1 JAN 64, WHICH IS OBSOLETE FOR ARMY USE.

Unclassified

Security Classification

14. KEY WORDS	LINK A		LINK B		LINK C	
	ROLE	WT	ROLE	WT	ROLE	WT
Elastic-rim wheels						
Off-road mobility						
Slope-climbing capability						
Slopes						
Wheels						

THE CONTENTS OF THIS REPORT ARE NOT TO BE USED FOR ADVERTISING, PUBLICATION, OR PROMOTIONAL PURPOSES. CITATION OF TRADE NAMES DOES NOT CONSTITUTE AN OFFICIAL ENDORSEMENT OR APPROVAL OF THE USE OF SUCH COMMERCIAL PRODUCTS.

FOREWORD

The study reported herein was conducted in 1970 as a part of Department of the Army Project 1T061102B52A, "Research in Military Aspects of Terrestrial Sciences," Task 01, "Military Aspects of Off-Road Mobility," under the guidance and sponsorship of the Research, Development and Engineering Directorate of the U. S. Army Materiel Command.

This was entirely a desk study conceived and carried out by Dr. K. W. Wiendieck, formerly of the Mobility Research Branch (MRB), Mobility and Environmental (M&E) Division, U. S. Army Engineer Waterways Experiment Station (WES), under the supervision of Messrs. W. G. Shockley and S. J. Knight, Chief and Assistant Chief, respectively, of the M&E Division. Data from a study previously conducted by the MRB for the National Aeronautics and Space Administration were used to verify the equations developed in this investigation.

COL Levi A. Brown, CE, and COL Ernest D. Peixotto, CE, were Directors of WES during this study, and Mr. F. R. Brown was Technical Director.

CONTENTS

CONVERSION FACTORS, METRIC TO BRITISH AND BRITISH TO METRIC UNITS OF MEASUREMENT

Units of measurement used in this report can be converted as follows:

Multiply	By	To Obtain
	Metric to British	
centimeters	0.3937	inches
square centimeters	0.1550	square inches
newtons	0.2248	pounds (force)
kilonewtons per square meter	0.1450	pounds per square inch
meganewtons per cubic meter	3.684	pounds per cubic inch
	British to Metric	
inches	2.54	centimeters
square inches	6.4516	square centimeters
pounds	4.4482	newtons

NOTATION

a	A constant, N^{-m}
A	Total area of contact surface, cm^2
A_d, A_z	Contributions to total contact area of wheel deflection and sinkage, respectively, cm^2
b	Width of test plate, cm
B	Wheel width, cm
c	Soil cohesion, kN/m^2
f	Coefficient, $cm\ N^{-1}$
G	Cone penetration resistance gradient, MN/m^3
k	A constant, $lb/in.^{2+n}$
k_c, k_ϕ	Bekker soil moduli, $lb/in.^{1+n}$ and $lb/in.^{2+n}$, respectively
K	Coefficient of deformability, $cm^2\ N^{-m/2}$
K_d, K_z	Coefficients of wheel and soil deformability, respectively, $cm^2\ N^{-m/2}$
ℓ	Wheel contact length, cm
m	A constant, dimensionless
n	A constant, dimensionless
P	Pull, N
P/W	Measured pull/load ratio, dimensionless
$(P/W)_o$	Maximum pull/load ratio on level ground (theoretical), dimensionless
r_c, r_i, r_n, r_s	Reduction factors applied to pull equation, dimensionless
r'_c, r'_n, r'_s	Modified reduction factors applied to pull equation, dimensionless
R	Undeflected wheel radius, cm
W	Wheel or axle load, N
W_i	Immobilization load, N

z	Sinkage, cm
δ	Wheel deflection, cm
θ	Angle of slope inclination, deg
θ'	Angle of additional slope due to sinkage, deg
$\theta'_c, \theta'_f, \theta'_i, \theta'_r$	Angle of additional slope due to sinkage on cohesive soil; on frictional soil; under corresponding rigid wheel under immobilization; and under a rigid wheel, respectively, deg
θ'_{max}	Angle of maximum frictional slope under rigid wheel, deg
K	Fraction of contact area due to sinkage, dimensionless
λ	Coefficient of slope-climbing capability, dimensionless
σ	Normal stress; pressure, kN/m^2
τ	Soil shear stress, kN/m^2
τ_c, τ_f	Cohesive and frictional components of shear stress, respectively, kN/m^2
ϕ	Angle of internal friction, deg

SUMMARY

The study reported herein is an effort to solve one of the problems of great significance in terrestrial mobility that was brought into focus by recent studies of lunar mobility, that of predicting wheel slope-climbing capability. Only empirical performance prediction techniques have been offered thus far. Therefore, an entirely new approach was attempted, which consisted of determining the pull performance of flexible wheels on yielding slopes by extrapolations. Two extrapolations were used, one starting from the theoretically known pull performance of flexible wheels on unyielding slopes, and the other from experimentally determined performance of rigid wheels on yielding, level ground. Thus, elements of both the theoretical and the empirical schools of thought were used in this semi-empirical approach. The result is a prediction equation for the available pull of elastic-rim wheels (as a particularly simple case of pneumatic tires) on deformable, inclined soils in terms of soil deformability, cohesion, and internal friction; wheel flexibility and load; and slope angle. The various reduction factors developed to take sinkage and load effects into account were adjusted to satisfy known conditions and to make the two extrapolations compatible.

It is recognized that the reasoning on which the extrapolations were based is mathematical rather than physical and that, therefore, the final equation lacks theoretical rigor. Nevertheless, this equation matches the extreme conditions on both ends of the soil and wheel deformability spectra with great accuracy and is, therefore, thought to describe intermediate conditions with a high degree of confidence. Of necessity, the equation has been checked numerically only for the test conditions provided by the lunar trafficability tests with elastic-rim wheels (Bendix wheel) because these wheels exhibited the simple deformation characteristics that were needed for this first formulation of a new approach. The more complex behavior of tires can be included later.

By solving this equation for zero pull, maximum slope-climbing capability can be determined; and by solving for zero slope, the maximum pull/load ratio on level ground can be obtained. In a proposed extension of the study, the solution of these two special cases will be combined into a dimensionless ratio, in which the inherent uncertainties will likely cancel out so that slope-climbing capability and the pull/load ratio will be linked in a satisfying manner.

PREDICTION OF THE SLOPE-CLIMBING CAPABILITY OF ELASTIC-RIM WHEELS

PART I: INTRODUCTION

Purpose

1. The purpose of this study was to develop by theoretical reasoning a method of predicting the slope-climbing capability of flexible wheels on yielding slopes with the slope material having both frictional and cohesive strength components. In particular, the study was aimed at providing a qualitative framework that would allow an optimum design for slope-climbing vehicles based on their maximum pull/load ratio determined experimentally on level ground. This study, prompted by lunar trafficability problems, has application to terrestrial problems as well.

Scope

2. The scope of the study was restricted by focusing on lunar vehicles and environments; specifically, only highly flexible wheels under light loads were considered. This restriction was dictated by circumstances that did not allow additional testing to broaden the scope. Quantitative reasoning was directed toward the Bendix wheel (fig. 1). This wheel

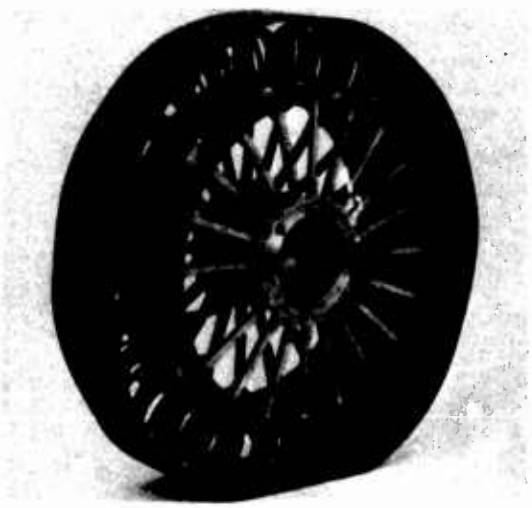

Fig. 1. Bendix wheel proposed for lunar vehicles

exhibits relatively simple deformation characteristics and produces a truly rectangular contact area, which greatly facilitated the analysis. Also, in accord with the known lunar soil data, only a relatively small amount of cohesion was considered in the numerical evaluations. However, the concept developed herein can be applied in principle to other wheels and other soils.

3. To simplify the study, only one-pass performance of grouserless wheels climbing uniform slopes was considered. Problems concerning wheel configurations or weight transfer are not discussed. The study was further limited by lack of funds; this prevented the use of a computer for presenting the results in a final form. However, this last step, which is necessary to complete the study, can be taken later.

PART II: THE BASIC CONCEPT

4. Since a new line of thought was explored in this investigation, a brief discussion of the basic concept, its underlying ideas, and its limitations is believed to be helpful. These are described in general terms in this part of the report.

5. For any powered running gear on unyielding surfaces, level or inclined, the available pull P can be computed theoretically. In fact, P depends only on the magnitude of the contact area A, the shear stresses τ in the direction of travel over this contact area, the angle θ of the slope, and the load W:

$$P = \tau A - W \sin \theta \qquad (1)$$

The term $W \sin \theta$ represents the load component parallel to the slope that reduces the total pull potential τA (fig. 2).

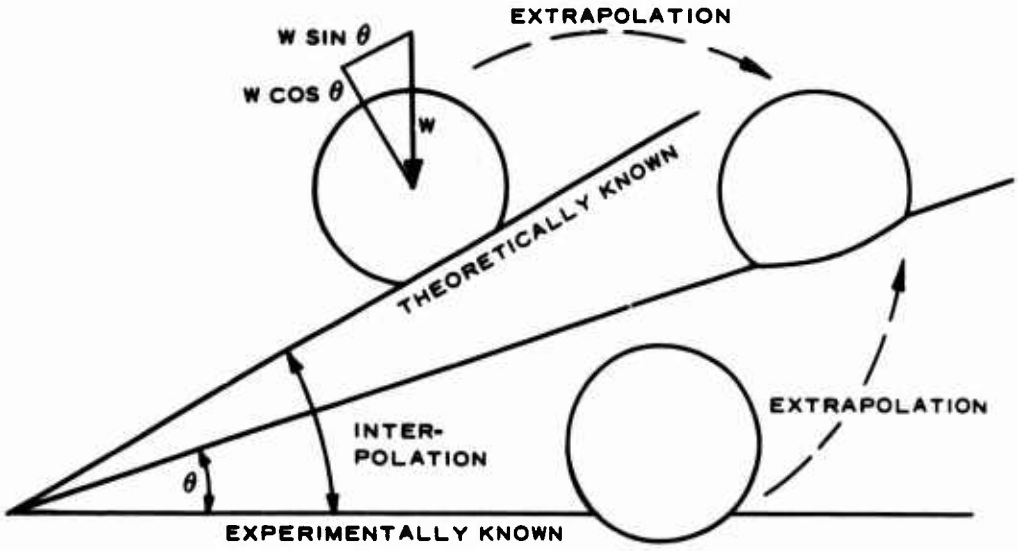

Fig. 2. Schematic illustration of semiempirical approach. Load components at top

6. The shear stress τ generally is composed of a frictional τ_f and a cohesive τ_c fraction:

$$\tau_c = c$$

$$\tau_f = \sigma \tan \phi = \frac{W}{A} \cos \theta \tan \phi \qquad (2)$$

where c is cohesion, σ is the average normal stress over the contact area, and ϕ is angle of internal friction.* The cosine term reflects the fact that only the load component normal to the slope can be taken into consideration. If sufficient slippage to fully activate total shear is assumed, τ_c and τ_f can be added according to the law of superposition; this is valid in this case of unyielding ground, since τ_c and τ_f refer to the same sliding surface, the contact area itself. Thus,

$$P = \left(\frac{W}{A} \cos \theta \tan \phi + c\right) A - W \sin \theta \qquad (3)$$

and

$$\frac{P}{W} = \tan \phi \cos \theta + \frac{cA}{W} - \sin \theta \qquad (4)$$

7. Solving equation 4 for level ground ($\theta = 0$) yields

$$\frac{P}{W} = \tan \phi + \frac{cA}{W} \qquad (5)$$

and solving it for slope-climbing capability ($P = 0$) yields

$$\tan \theta = \tan \phi + \frac{cA}{W} \cos \theta \qquad (6)$$

By using the trigonometric relation $\cos \theta = 1/\sqrt{1 + \tan^2 \theta}$, equation 6 can be solved explicitly for θ:

$$\tan \theta = \frac{W^2}{W^2 - c^2A^2}\left(\tan \phi + \frac{cA}{W^2}\sqrt{W^2 - c^2A^2 + W^2 \tan^2 \phi}\right) \qquad (7)$$

---

* In view of the later extrapolation and for consistency, soil-related terms cohesion and internal friction are used here instead of adhesion and coefficient of friction. The soil-wheel interaction in this case of unyielding soil can be visualized as the sliding of an infinitesimal soil layer.

A comparison of equations 5 and 7 shows that even on unyielding surfaces, the assumption $\tan \theta = P/W$ that has been used for a rough prediction of slope-climbing capability is not theoretically valid.* For an unyielding surface possessing both frictional and cohesive properties, there are only two cases for which $P/W = \tan \theta$ is valid. These are:

a. $A = 0$ (point contact, rigid wheel).

b. $A = fN$ (where f is simply a coefficient and N is normal load, i.e. W on level ground, $W \cos \theta$ on a slope).**

8. The approach followed in this report consists in identifying and quantifying complementary corrective terms, which are then evaluated with regard to $P/W = \tan \theta$. Since this equation is valid for rigid wheels on unyielding surfaces, two groups of corrective terms are distinguished:

a. Those resulting from the wheel deformation.

b. Those resulting from soil deformation.

9. Identification and quantification of terms in the first group do not present major difficulties; there is, in fact, only a question of the mathematical formulation of the load-contact area relation $A = f(W)$ on unyielding ground. Depending on the complexity of this relation, a number of parameters can be identified and quantified by simple loading tests. Whenever the $A = f(W)$ relation is known, A can be eliminated from the pull equation (equation 3). With $\theta = 0$ or $P = 0$, both the maximum pull/load ratio on level ground (equation 5) or the slope-climbing capability (equation 7) can be determined theoretically for unyielding surfaces in terms of ϕ, c, W, and the flexibility parameters of the wheel.

---

* It should be noted, however, that the assumption $P/W = \tan \theta$ is fairly good. In a soil where cohesion $c = 0$, $\cos \theta = 1$ and P/W (equation 5) = $\tan \theta$ (equation 6) = $\tan \phi + cA/W$. In a soil with a finite value of c, the discrepancy, of course, depends on specific values of c, ϕ, A, W, and θ. The worst case is the one in which θ is high and ϕ is zero. If the highest θ practicable (35 deg) and $\phi = 0$ are assumed, the discrepancy would be 22 percent ($P/W = cA/W$ (equation 5) versus $\tan \theta = cA/W \cos 35 \text{ deg} = 1.22\, cA/W$ (equation 6)). Since soil lying on a relatively steep slope would undoubtedly show a significant ϕ value, the actual discrepancy in assuming $P/W = \tan \theta$ would not appear to be very great (probably less than 10 percent) in practical situations.

** This point is proven easier by equation 6 than by equation 7.

The relative simplicity of the $A = f(W)$ relation for the Bendix wheel* was a major reason for using this wheel in the numerical evaluation.

10. The corrective terms associated with soil deformation, or wheel sinkage, are less easily assessed. To arrive at a workable solution, sinkage was considered to have seven distinguishable effects on available pull on slopes:

a. Increase in the size of the contact area.

b. Increase in forward part of the contact area due to bow wave.

c. Decrease in rearward part of contact area due to nonelastic soil behavior.

d. Decrease in rearward part of the contact area due to a tendency of soils on slopes to slide off behind the wheel.

e. Reduction of pull-generating shear stress resultant due to curvature of contact area.

f. Reduction of theoretical shear stress potential due to complex rupture phenomena within the soil.

g. Inapplicability of the superposition principle.

A detailed discussion of these effects is presented in paragraphs 24-42.

11. A correction term is associated with each of these effects and is applied to the theoretical pull equation for the Bendix wheel on unyielding slopes. Generally, these corrective terms are simple functions containing one or more parameters. Both the mathematical formulation of these functions and the assignment of numerical values to their parameters constitute the quantification of the sinkage-related corrective terms. It is emphasized that this quantification is based on consideration of known or assumed trends and mathematical simplicity, in combination with general reasoning, rather than on physical insight into the complex mechanism of the soil-wheel interaction. This is a major weakness of the approach, but the lack of a sound theoretical concept did not allow proceeding otherwise.

12. Thus, the approach consists basically of a step-by-step extrapolation to the unknown pull performance of flexible wheels on yielding slopes, starting from the theoretically known pull equation on unyielding

---

* This relation is even simpler for a track on unyielding ground: A = constant; however, tracks are not considered for lunar vehicles.

slopes. The inherent danger of this procedure is immediately obvious, since extrapolations into the unknown acquire more purely speculative elements the further they go. Therefore, to keep the degree of conjecture within tolerable limits, as many control mechanisms as possible must be incorporated in the system.

13. In this study a major control is provided by the experimentally known pull performance of wheels on yielding level ground, particularly that of rigid wheels. The individual terms as well as the final equation were checked as far as possible in this respect. In a sense, the extrapolation procedure was thus complemented and controlled by an interpolation between the extreme cases of a flexible wheel on unyielding ground and a rigid wheel on yielding ground. This is schematically represented in fig. 2.

14. In addition, the numerical values of the various parameters were chosen, whenever possible, to correspond to known extreme cases, or "fix points." These fix points will be pointed out in the following text as they appear. In general, the procedure consists of linking such fix points by equations that satisfy the extreme conditions and are felt to describe the intermediate conditions in an acceptable manner.

15. Thus, in essence, the proposed approach represents a network of extrapolations and interpolations that are suspended at various fix points to give the network some stability. Admittedly, this network is rather tenuous, and the approach might be described less positively as a system of speculation and conjecture. However, the built-in control mechanisms should give it some degree of credence and should yield at least a qualitative picture of the problem. In other words, this study does not show what is, but what possibly could be; and if the reasoning is not based strictly on physical laws, physical laws at least are not violated.

16. Finally, in a possible extension of this study, the results can be represented by a dimensionless ratio $\lambda = \tan\theta/(P/W)_o$, where $(P/W)_o$ is the maximum pull/load ratio on level ground as determined by equation 4. Since both the numerator and the denominator of the λ ratio represent extreme cases of equation 4, there is an increased chance for the inherent uncertainties to cancel out. By having a computer determine the numerical

λ value for various sets of parameters, a good feel for the actual λ value will be obtained. The prediction of the slope-climbing capability of wheels then becomes possible by using the formula $\tan \theta = \lambda(P/W)$, where P/W is the ratio of actually measured pull and load on level ground as opposed to the theoretical $(P/W)_o$ value.

PART III: DEVELOPMENT OF PULL EQUATION FOR ELASTIC-RIM WHEELS

Pull on Unyielding Slopes

17. For the purpose of this study, an elastic-rim wheel is defined as one with a central axle, intermediate components including those for suspension, and an outer rim of constant width that is extremely flexible in the direction of travel and totally inflexible in the lateral direction. Therefore, the contact area under such a wheel is rectangular on unyielding surfaces and will vary as a function of load only in the direction of travel. The Bendix wheel (fig. 1) and the Grumman wheel without grousers (fig. 3) qualify as elastic-rim wheels.

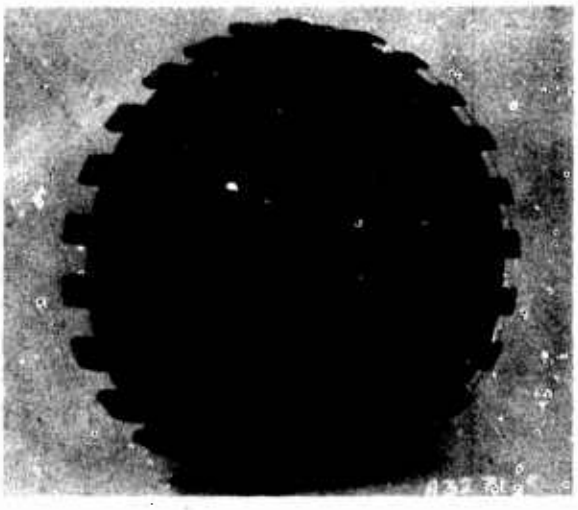

Fig. 3. Grumman wheel proposed for lunar vehicles

18. Such wheels can be assumed to exhibit load-deflection characteristics of the general form*

$$\frac{\delta}{R} = aW^m \tag{8}$$

where δ is deflection of the wheel, R the undeflected wheel radius, W the axle load, and m and a are characteristic constants. The actual

---

* Any other general form that describes load-deflection characteristics adequately, e.g. a hyperbolic function, could be chosen for equation 8.

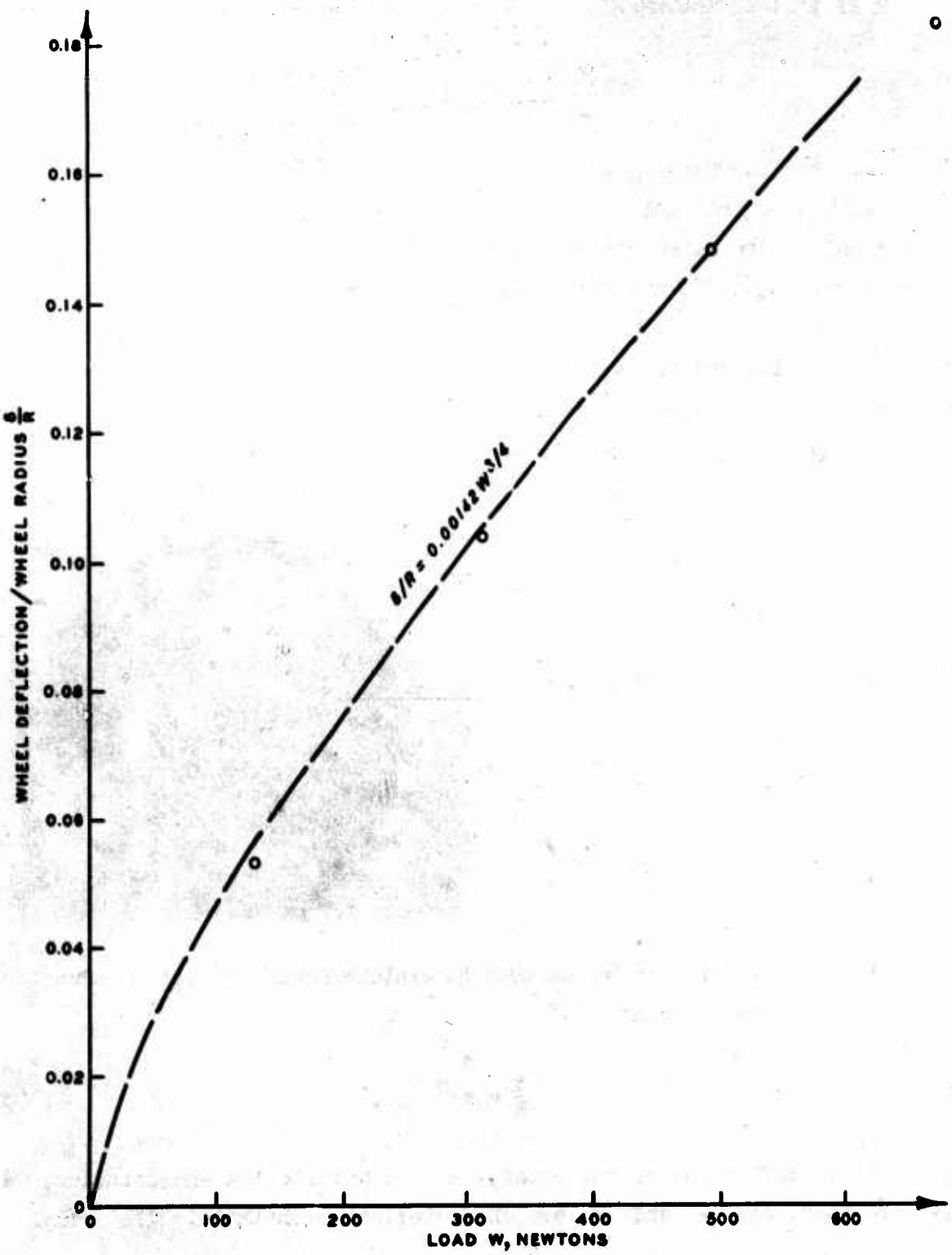

Fig. 4. Load-deflection curve for Bendix wheel

Note: A table of factors for converting metric to British and British to metric units of measurement is presented on page xi.

load-deflection relation for the Bendix wheel is shown in fig. 4, together with the analytical function

$$\frac{\delta}{R} = 0.00142W^{3/4} \tag{9}$$

which almost perfectly matches the experimental values. For the sake of generality, however, equation 8 will be used.

19. The contact length ℓ of the deflected wheel is assumed to be the length of the chord in the circle defined by deflection δ in fig. 5.

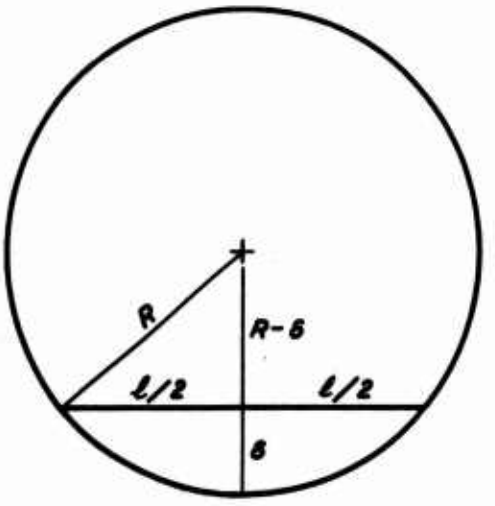

Fig. 5. Chord of circle as contact length

Hence

$$(R - \delta)^2 + \frac{\ell^2}{4} = R^2$$

$$\ell^2 = 8R\delta - 4\delta^2 \approx 8R\delta$$

$$\ell = R\sqrt{8\frac{\delta}{R}} \quad \text{(for small deflections, e.g. } \delta/R \ll 0.1) \tag{10}$$

Introducing equation 8 and multiplying by width B of the wheel yields the contact area:

$$A_d = RB\sqrt{8aW^m} = K_d W^{m/2} \tag{11}$$

if all wheel parameters are combined in the constant

$$K_d = RB\sqrt{8a} \tag{12}$$

The subscript d stands for wheel deformation. On slopes, only the normal load component $W \cos \theta$ (fig. 2) contributes to the deflection; therefore, the general expression for the contact area under elastic-rim wheels is

$$A_d = K_d \sqrt{(W \cos \theta)^m} \tag{13}$$

20. Introducing equation 13 into the general pull equation 3 results in the pull equation for elastic-rim wheels on unyielding slopes:

$$P = W \cos \theta \tan \phi + K_d c \sqrt{W^m} \sqrt{\cos^m \theta} - W \sin \theta \tag{14}$$

The pull/load ratio on level ground is obtained by solving for $\theta = 0$:

$$P/W = \tan \phi + K_d c \sqrt{W^{m-2}} \tag{15}$$

The corresponding slope-climbing capability equation ($P = 0$) leads to the expression

$$\tan \theta = \tan \phi + K_d c \sqrt{W^{m-2}} \sqrt{\cos^{m-2} \theta} \tag{16}$$

21. In these general forms, neither equation 15 nor equation 16 is solvable explicitly for P/W or $\tan \theta$, respectively, except in two hypothetical cases:

a. $K_d = 0$ (i.e. $A = 0$): $P/W = \tan \phi$, $\tan \theta = \tan \phi$

b. $m = 2$: $P/W = \tan \phi + K_d c$, $\tan \theta = \tan \phi + K_d c$

In both cases, the slope-climbing capability is equal to the P/W ratio on level ground.*

22. Nevertheless, a comparison of equations 15 and 16 yields an important result. Generally, the slope-climbing capability of elastic-rim wheels on unyielding surfaces is larger than the P/W ratio on level ground because $\sqrt{\cos^{m-2}\theta} > 1$ for $m < 2$.** Hence, the slope-climbing factor as defined in paragraph 16 is

$$\lambda = \frac{\tan\theta}{(P/W)_o} = \frac{\tan\phi + K_d c\sqrt{W^{m-2}}\sqrt{\cos^{m-2}\theta}}{\tan\phi + K_d c\sqrt{W^{m-2}}} > 1 \qquad (\text{for } m < 2)$$

23. Since the term $\sqrt{\cos^{m-2}\theta}$ is associated with cohesion c, the neglect of cohesion could lead to an underestimate of the slope-climbing capability on the basis of a known P/W ratio. The commonly used approximation $\tan\theta = P/W$, resulting in $\lambda = 1$, does not contain provisions for including the possibly decisive effects of cohesion.

Extrapolation to Yielding Slopes

Quantification of sinkage effects

24. Wheel sinkage is a complex mechanical process, and its net effect undoubtedly is a decrease in a wheel's slope-climbing capability on yielding surfaces. It is, however, impossible to quantify the overall effect on a sound basis, so the sinkage problem was split into manageable portions as itemized in paragraph 10. This breakdown does not follow entirely the lines of physical reasoning (for which a better insight into the process itself would have been needed), but rather is based on the geometry of the contact area, which is itself a result of the soil-wheel interaction. Thus, paragraph 10a deals with the size of the total contact area; paragraphs 10b, 10c, and 10d deal with the proportion of its forward

---

* Both cases correspond to those already discussed in paragraph 7. Equation 13 shows that $m = 2$ yields a linear normal load-contact area relation.

** For the Bendix wheel $m = 0.75$ (fig. 4).

and rearward parts with respect to the total; and paragraph 10e deals with its curvature. Only paragraphs 10f and 10g refer directly to the physics of the matter. Nevertheless, this somewhat inconsistent procedure permits covering the entire sinkage complex without overlapping and without major gaps.

25. Effect of sinkage on size of contact area. (See paragraph 10a.) With increasing soil deformability or decreasing wheel flexibility, the size of the contact area depends more and more on sinkage. Introducing the extreme case of a rigid wheel on yielding ground as a fix point and assuming the contact length of the rigid wheel as the chord of a circle* (fig. 5) yields the following expression for the contact area:

$$A = \ell \cdot B \approx B\sqrt{8Rz} \tag{17}$$

in which sinkage z has been substituted for deflection δ. To eliminate sinkage from this expression, a suitable pressure-sinkage relation must be introduced. A commonly used equation** is

$$\sigma = kz^n \tag{18}$$

where

σ = pressure

z = sinkage

k,n = constants

If $\sigma = W/A$ and equations 17 and 18 are combined, after some lengthy procedures,

$$A = \frac{(B\sqrt{8R})^{2n/(2n+1)}}{k^{1/(2n+1)}} W^{1/(2n+1)} \tag{19}$$

---

* It is fully realized that this assumption is valid only for relatively small sinkages.

** As in the case of equation 8, this equation represents only one of numerous possibilities for describing the relation between static loading and deformation for a specific soil. Its use here does not exclude the use of any other function, e.g. a hyperbola,[1,2] which might describe the relation better.

Grouping the soil and wheel constants into one constant K_z and making

$$\bar{m} = \frac{2}{2n + 1} \tag{20}$$

transform equation 19 into

$$A_z = K_z W^{\bar{m}/2} \tag{21}$$

where z stands for sinkage, and

$$K_z = \frac{(B\sqrt{8R})^{(2-\bar{m})/2}}{k^{\bar{m}/2}} \tag{22}$$

26. Equation 21 has the same form as equation 11, a parallel that allows the treatment of sinkage effects in the same manner as deflection effects. This agreement is essential in the following analysis. Besides this more formal point, a quantitative parallel also exists between equations 11 and 21, in that the exponents m (equation 11) and $\bar{m}$ (equation 21) can reasonably be assumed to have about the same numerical value. In fact, the exponent n of the pressure-sinkage equation (equation 18) usually has values between 1/2 and 1,* yielding (equation 20) $\bar{m} = 1$ and $\bar{m} = 2/3$, respectively. The exponent m in the load-deflection relation (equation 11) is also smaller than unity for elastic-rim wheels and can be assumed to vary for various wheels in the range of 0.5 to 1.0. Thus, $2/3 < \bar{m} < 1$ for equation 21, and $1/2 < m < 1$ for equation 11. It can therefore be assumed in the framework of this general evaluation that the exponent m has the same numerical value in both equations ($m = \bar{m}$), and in particular, $m = 3/4$ in regard to the Bendix wheel (paragraph 18 and fig. 4).

27. When $m = \bar{m}$ is assumed,** the difference in the contribution of sinkage and deflection to the contact surface resides in the magnitude of the constants K_d and K_z alone (equations 11 and 21). These constants

---

* The simplifying value $n = 0$ that is sometimes assumed is unrealistic.
** There will be no further distinction between m and $\bar{m}$.

represent the deformability of the wheel and of the soil, respectively. Designating by A_z and A_d the contributions of wheel sinkage and deflection, respectively, to the total contact area $A(A_z + A_d)$, and assuming A_z and A_d to be proportional to the respective deformability constants K_z and K_d, yield

$$A_d = A \frac{K_d}{K_d + K_z} \quad ; \quad A_z = A \frac{K_z}{K_d + K_z} \tag{23}$$

where the total area is

$$A = (K_z + K_d) W^{m/2} \cos^{m/2} \theta \tag{24}$$

which is a generalization of equation 13. The abbreviation

$$\kappa = \frac{K_z}{K_z + K_d} \tag{25}$$

furnishes a convenient expression for that fraction of the contact area that is due to sinkage, while the complementary expression $1 - \kappa = K_d / (K_z + K_d)$ designates the fraction resulting from wheel flexibility. Thus, $\kappa = 0$ indicates an unyielding surface, $\kappa = 1$ a rigid wheel on a yielding surface, and $\kappa = 0.5$ an equal contribution to the size of the contact area of both the wheel and the soil deformation.

28. The numerical value of κ can be computed in terms of wheel dimensions (B, R), load-deflection (a), and pressure-sinkage (k) parameters for an assumed or given exponent m. By using the appropriate definitions (equations 12 and 22),

$$\kappa = \frac{K_z}{K_d + K_z} = \frac{\sqrt{(B\sqrt{8R})^{2-m}}}{RB\sqrt{8a}\sqrt{k^m} + \sqrt{(B\sqrt{8R})^{2-m}}} \tag{26}$$

The unyielding surface is defined by $k \to \infty$, resulting in $\kappa = 0$, and the rigid-wheel condition ($a = 0$) results in $\kappa = 1$.

29. Increase of forward part and decrease of rearward part of contact area. (See paragraphs 10b, 10c, and 10d.) Presence of a bow wave, the nonelasticity of the soil, and the tendency for soil to slide off behind the wheel act together in that they make the wheel climb a steeper slope. The angle of this additional slope θ' is defined as the angle between the line connecting the forward and rearward edges of the contact area and the slope line (fig. 6). The angle θ' is greater for frictional

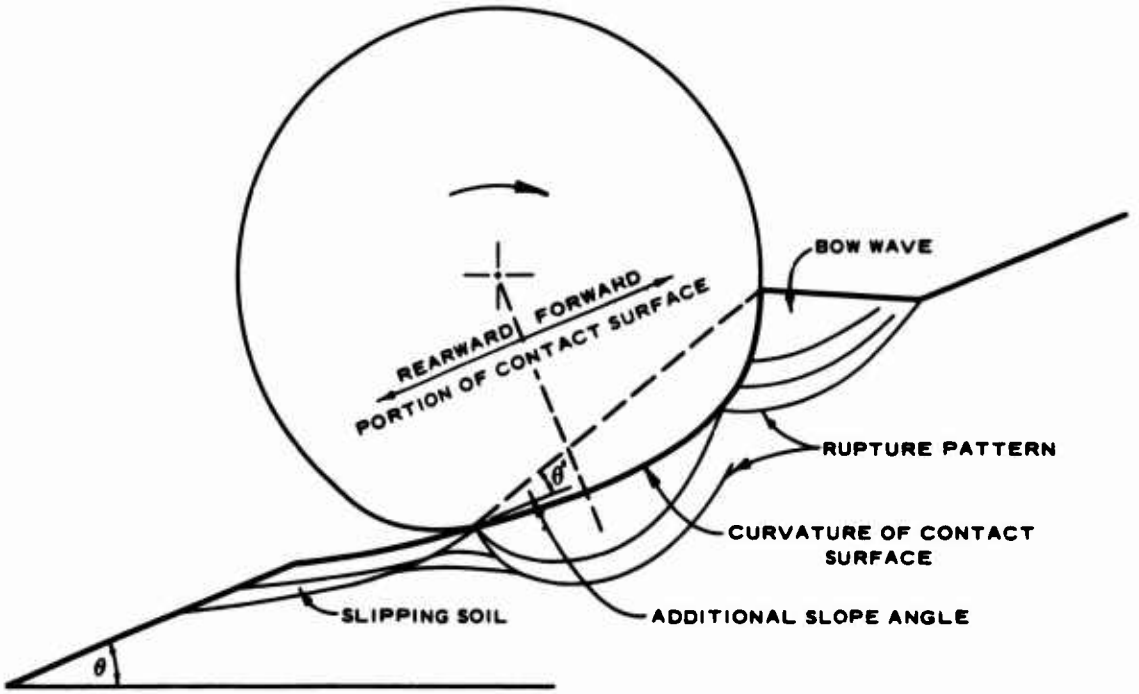

Fig. 6. Sinkage effects

soil than for cohesive soil because much larger bow waves have been observed in sands than in clay and because granular material tends to slip from behind the wheel on slopes much easier than cohesive material. These effects were therefore separated into frictional and cohesive components.*

30. For a purely frictional material, the following fix points can be identified:

---

* In a later modification of the system, this differentiation was abandoned.

a. $K = 0$ (hard surface).

No effect: $\theta' = 0$.

b. $K = 1$, $\theta = \phi$ (rigid wheel on maximum frictional slope).

Maximum effect: $\theta' = \theta'_{max}$.

c. $K = 1$, $\theta = 0$ (rigid wheel on level ground).

θ'_r can be determined from tests.

Assumedly, the difference in θ' for conditions b and c , above, is rather small because it stems uniquely from the supposedly slightly higher bow wave at the front end and the sliding of sand at the rear end of wheels on slopes.

31. The three extreme conditions are fulfilled by:

$$\theta' = K\left[\frac{\theta}{\phi}\,\theta'_{max} + \left(1 - \frac{\theta}{\phi}\right)\theta'_r\right] \qquad (27)$$

The magnitude of θ'_{max} and θ'_r , both of which refer to a rigid wheel (paragraphs 30b and 30c), depends on such factors as axle load, wheel dimensions, slip, and soil strength. It is impossible to take all these parameters properly into account. Soil strength is somewhat superficially incorporated in the K value; and it is felt that load and wheel dimensions do not greatly influence θ' because sinkage and contact length, which chiefly determine θ'_r , vary roughly in the same proportions for rigid wheels, regardless of load and wheel dimensions. Finally, there is no need to consider the whole slip range in conjunction with slope-climbing capability, since only the maximum P/W ratio at about 20 percent slip is of interest. In any case, θ'_r is an experimental parameter that can be determined easily for a given condition.

32. The geometric configuration of a towed, highly inflated tire (fig. 7) is used as a guide to tentatively quantify equation 27. With reference to the undeformed tire outline, θ'_r is measured to be 23 deg when the bow wave is taken into account and 18 deg when it is not. If a slightly larger bow wave for condition b (paragraph 30) is assumed and the rearward

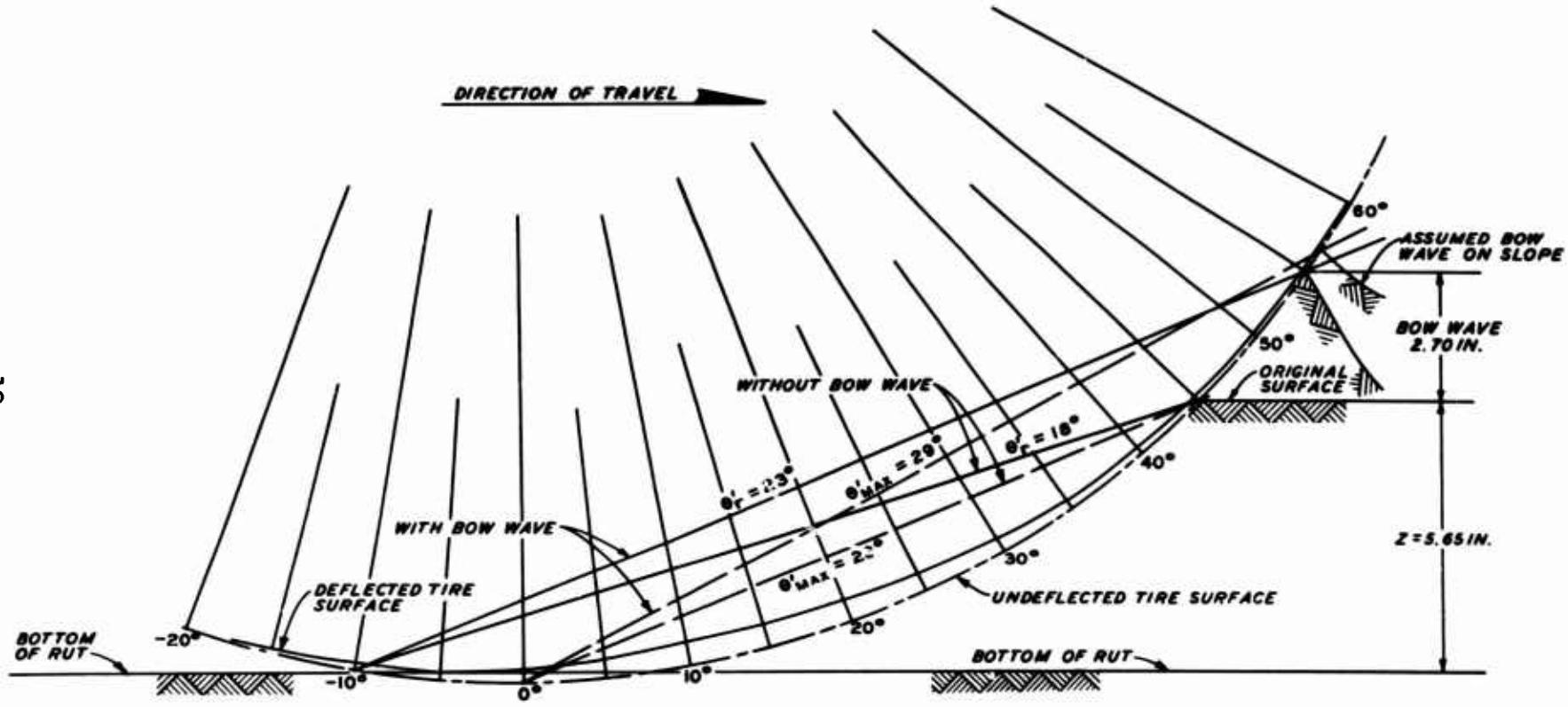

Fig. 7. Determination of various additional slope angles (adapted from reference 3)

end of the contact area coincides with the bottom dead center, in this extreme case θ'_{max} is 29 deg and 23 deg with and without inclusion of the bow wave, respectively. With a somewhat smaller bow wave for the 20 percent slip condition, θ'_r and θ'_{max} have intermediate values and may be assumed to be: $\theta'_r = 20$ deg and $\theta'_{max} = 25$ deg $= 1.25\ \theta'_r$. When these values are substituted in equation 27,

$$\theta'_f = K\theta'_r \left(1 + 0.25 \frac{\theta}{\phi}\right) \tag{28}$$

where f stands for friction.

33. For $\theta'_r = 20$ deg, equation 28 yields reasonable quantitative values. For example, if $K = 0.5$ for a low-inflated tire in otherwise identical conditions, as previously discussed (fig. 7), $\theta'_f = 10$ deg, which is in agreement with fig. 8; and for the even more flexible Bendix wheel with an estimated value of $K = 0.2$,* $\theta'_f = 4$ deg, which agrees well with what was observed. However, a more precise estimate for a particular wheel, such as the Bendix wheel, under defined loading and soil strength conditions can be obtained by measuring θ'_r directly with a rigid version of the wheel.

34. For cohesive soils, bow wave effects are almost nonexistent. Also, the sliding-off effect of soils behind the wheel on slopes is assumed to be insignificant. Therefore,

$$\theta'_c = K\theta'_r \tag{29}$$

where c is cohesion and θ'_r can be assumed from fig. 7, for the purpose of this study, to be 18 deg. For more precise estimates, this angle should be measured with a rigid wheel.

35. Curvature of contact area. (See paragraph 10e.) As a result of the curvature of the contact area, neither the pull-generating shear stresses nor their resultant act in the direction of travel. This effect decreases with the deformability K_d of the wheel and increases with that

* Numerical examples in paragraph 50 show that $K = 0.2$ for the Bendix wheel is a reasonable assumption.

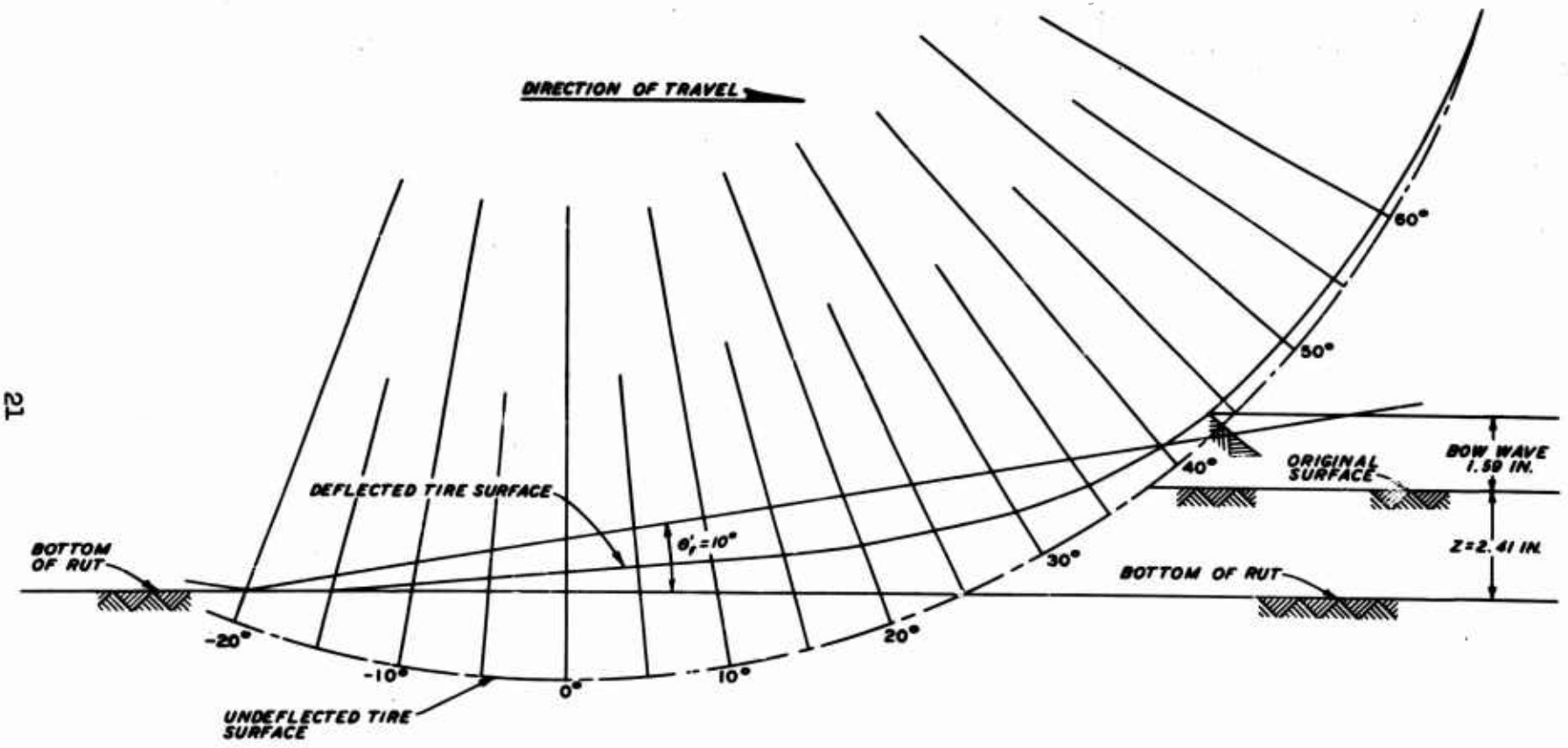

Fig. 8. Additional slope angle θ' for low-inflated tire on sand (adapted from reference 3)

of the soil K_z. With r_c designated the reduction factor due to curvature, fix points are evaluated as before:

a. $r_c = 1$ for $K_z = 0$ ($\kappa = 0$), i.e. no reduction on unyielding surfaces.

b. $r_c = r_{c_{min}}$ for $K_d = 0$ ($\kappa = 1$), i.e. highest reduction for rigid wheels.

36. The second condition is the most unfavorable one, but it is felt that the reduction even in this case is rather small, about 10 percent under normal sinkage conditions. If it is assumed that r_c is independent of slope and soil type and that it is linearly related to the relative soil deformability κ as was previously done, it is postulated that

$$r_c = 1 - 0.1\kappa \tag{30}$$

Thus, for a highly flexible wheel, such as the Bendix, with an assumed value of $\kappa = 0.2$, the effect is insignificant: $r_c = 0.98$.

37. Reduction of shear stress potential at the contact area. (See paragraph 10f.) The maximum shear stress a soil can sustain is given by Coulomb's law $\tau = c + \tan \phi$. Since this equation is valid only along real or potential rupture lines within the soil, it can be applied directly toward wheel performance prediction only if the soil-wheel interface is a real or potential rupture surface. This is generally not the case. For rigid wheels on sand ($c = 0$), it was found[4,5] that the theoretical shear stress potential $\tau = \sigma \tan \phi$ was utilized at the soil-wheel interface only at about half rate, varying roughly between 35 and 65 percent at 20 percent slip, the higher values being associated with a narrow wheel and low soil strength.*

38. Physically, these variations reflect variations in the rupture pattern, about which practically nothing is known insofar as flexible wheels are concerned. In an extreme simplification, it can be assumed that the

---

* In references 4 and 5 this result is presented in terms of the mean shear-to-normal stress ratio $t_m = \tau/\sigma$, which was not directly measured. When extreme variations are neglected, most of the t_m values were found to vary between 0.35 tan ϕ and 0.65 tan ϕ.

degree of utilization of shear stress potential increases with the degree of confinement of the rupture pattern to the immediate neighborhood of the soil-wheel interface. Three fix points can thus be defined for which the rupture pattern coincides with the contact surface and for which, consequently, the shear stress potential is utilized 100 percent. These points are:

a. 100 percent slip condition.

b. Zero contact length (zero load) condition.

c. Unyielding soil condition ($K = 0$).

39. The 100 percent slip condition is irrelevant in the study of slope-climbing capability and is, therefore, eliminated from consideration. A slip of 20 percent is assumed for maximum slope-climbing capability. Also, it is felt that the reduction in the pull due to the effect of underdeveloped shear stress decreases with slope. This point is perhaps elucidated by considering a 90-deg slope, which yields a zero contact area for all cases, i.e. full (hypothetical) utilization of the shear strength potential.

40. If once more the rigid wheel condition on level ground is assumed to be the worst, with a reduction factor of 50 percent at 20 percent slip (i.e. roughly the mean value between the measured 35 and 65 percent limits)[4,5] the considerations above lead to the expression

$$r_s = 1 - 0.5K \cos \theta \qquad (31)$$

where s stands for stress. The dependency of r_s on slope angle is assumed to be adequately expressed by the cosine term. For $\theta = 90$ deg, $r_s = 1$ (i.e. no reduction). Since comparable studies of rigid wheels on clay have not yet been conducted, the same relation is assumed to be applicable to the contribution of cohesion to slope-climbing capability of wheels. That is, of necessity, only a very rough evaluation of this important effect, and a refinement of equation 31 certainly will be possible as a result of further basic research on soil-wheel interaction, especially on soil rupture patterns.

41. Inapplicability of superposition principle. (See paragraph 10g.)

Since the simple addition of independent cohesive and frictional effects on pull yields the maximum total effect, the inapplicability of superposition constitutes a performance reduction with respect to the theoretical maximum. The magnitude of this effect can only be guessed, but it is believed that it is not too important. Since the same fix points (paragraph 38) apply here, i.e. that the effect is nil for 100 percent slip, for zero contact length, and for unyielding soil, and since the same general reasoning as to the variation of this effect (paragraph 39) is valid, the reduction formula for this effect is developed along the same lines.

42. However, this reduction is applicable only if superposition is actually made, i.e. if the soil indeed has frictional and cohesive properties. If the reduction factor is maximum when the frictional shear strength component $\sigma \tan \phi$ and the cohesive component c are equal, and if this case yields about 25 percent reduction for a rigid wheel, the reduction due to inapplicability of the principle of superposition r_n* is described by

$$r_n = 1 - 0.25\kappa \cos \theta \frac{2\sqrt{c\sigma \tan \phi}}{c + \sigma \tan \phi} \tag{32}$$

which satisfies the above-listed requirements. The mean contact pressure σ can be expressed by using equation 24:

$$\sigma = \frac{W \cos \theta}{A} = \frac{W \cos \theta}{(K_z + K_d)(W \cos \theta)^{m/2}} = \frac{\sqrt{(W \cos \theta)^{2-m}}}{K_z + K_d} \tag{33}$$

Assemblage of pull equation

43. The first formulation of the pull equation is developed from equation 14, in which the first term represents the frictional part, the second the cohesive part, and the third the weight component to be pulled upslope. Additional slope angles θ_f' and θ_c' (paragraphs 32 and 34) are incorporated in the first two terms, but not the third term. Also, the

* The reduction r_n describes well the experimental finding that "with increasing cohesion, the rate of increase of pull decreases."[6] In fact, the reduction factor r_n decreases with increasing cohesion (until the condition $c = \sigma \tan \phi$ is reached), the net result being that the increase in cohesion is not fully reflected in the increase in the P/W ratio.

various reduction factors r_c, r_s, and r_n (paragraphs 35-42) are applied only to the first two terms of equation 14. Finally, K_d must be replaced by $K_d + K_z$ on yielding soils:

$$P = r_c r_s r_n \left[W \cos (\theta + \theta_f') \tan \phi + (K_z + K_d)\, c \sqrt{W^m \cos \left(\theta + \theta_c'\right)^m} \right] - W \sin \theta \qquad (34)$$

where

$r_c = 1 - 0.1\kappa$ (equation 30)

$r_s = 1 - 0.5\kappa \cos \theta$ (equation 31)

$r_n = 1 - 0.5\kappa \cos \theta \dfrac{\sqrt{c\sigma \tan \phi}}{c + \sigma \tan \phi}$ (equation 32)

$\kappa = \dfrac{\sqrt{(B\sqrt{8R})^{2-m}}}{RB\sqrt{8a}\sqrt{k^m} + \sqrt{(B\sqrt{8R})^{2-m}}}$ (equation 26)

$\sigma = \dfrac{\sqrt{(W \cos \theta)^{2-m}}}{K_z + K_d}$ (equation 33)

$K_z = \dfrac{\sqrt{(B\sqrt{8R})^{2-m}}}{\sqrt{k^m}}$ (equation 22)

$K_d = RB\sqrt{8a}$ (equation 12)

$\theta_f' = \kappa\left(1 + 0.25 \dfrac{\theta}{\phi}\right)20$ deg (equation 28)

$\theta_c' = \kappa\ 18$ deg (equation 29)

44. The pull/load ratio on level ground ($\theta = 0$) then is

$$\frac{P}{W} = r_c r_s r_n \left[\cos \theta_f' \tan \phi + (K_z + K_d)\, c \sqrt{W^{m-2} \cos^m \theta_c'} \right] \qquad (35)$$

and the implicit expression for the maximum slope-climbing capability is obtained from equation 34 by making $P = 0$.

45. Equation 34 is a semitheoretical expression for predicting the available pull of flexible wheels on yielding slopes. It is semitheoretical

because only its skeleton is strictly theoretical, while the complementary terms are based on qualitative reasoning, intuition, and some experimental data. However, for the extreme condition of unyielding soils ($K = 0$), equation 34 and the expressions derived from it are rigorous in that they become identical with those derived by purely theoretical means for unyielding surfaces.

46. These equations can, therefore, be expected to yield reasonably accurate results in the range of low K values. Since K describes the relative deformability of the soil with respect to that of the soil-wheel system, low K values are obtained not only for a low soil deformability, but also for a high wheel deformability, which is characteristic for the lunar wheels. For the Bendix wheel on medium dense sand, $K < 0.2$ can be assumed, and numerical checks of equation 35 against test results support its validity in the range of low K values for which it was originally developed (paragraphs 48-56).

47. The amount of extrapolation inherent in these equations is indicated by the K value. The highest K value ($K = 1$) indicates maximum extrapolation for the rigid wheel on yielding soils, in which case the equations have the least degree of reliability. In accordance with the general concept to "anchor" these equations at all possible fix points, equation 35 will also be checked against rigid wheel ($K = 1$) performance that has been experimentally determined.

Numerical Verification

48. Since single-wheel tests on slopes have not been performed, the numerical examples will refer to the special case of zero slope (equation 35).

Determination of K

49. The K value depends both on wheel characteristics and on soil properties in terms of a plate sinkage test. However, within the framework of the lunar trafficability study,[6] plate sinkage tests were made only occasionally. Furthermore, the K value can be determined numerically only under the assumption of m having the same value in equations 11 and 21,

particularly $m = 0.75$ (paragraph 26). This corresponds to a value of $n = 0.833$ for the exponent of the original pressure-sinkage equation (equation 18) because of the substitution given by equation 20. Therefore, the exact κ value can be determined for only the few cases wherein the exponent n, as determined from plate sinkage tests, happened to be about 0.833. In connection with the first-pass Bendix wheel tests, this occurred only once, in test 11 where n was measured to be 0.89, and k_ϕ and k_c were 3.5 $lb/in.^{2+n}$ and -0.43 $lb/in.^{1+n}$, respectively (table 2 of reference 6).

50. If the negligibly small k_c value, which should be 0 anyway for this air-dry sand (S_1 condition), is ignored, the order of magnitude of κ is evaluated for the following numerical values:*

$R = 20$ in.

$B = 10$ in.

$a = 0.00142\ N^{-m}$

$k = k_\phi = 3.5\ lb/in.^{2+n} = 15.6\ N/in.^{(3n+2)/2m}$**

$n = 0.75 = 3/4$

This results in (equation 12):

$$K_d = RB\sqrt{8a}$$

$$= 20 \cdot 10 \cdot \sqrt{0.01135} = 21.3 \quad (in.^2\ N^{-m/2})$$

and (equation 22)

$$K_z = \frac{(B\sqrt{8R})^{(2-m)/2}}{k^{m/2}}$$

$$= \frac{(10 \cdot 12.64)^{5/8}}{15.6^{3/8}} = 7.35 \quad (in.^2\ N^{-m/2})$$

---

* In reference 6, the Bekker equation $p = (k\phi + k_c/z)^n$ was used to evaluate the plate sinkage tests. For $c = k_c = 0$, $k = k\phi$ (compare with equation 18). For $c \neq 0$ and $k_c \neq 0$, $k = (k\phi + k_c/b)$ and is dependent on plate width.

** These somewhat odd dimensions were convenient for use in intermediate calculations.

yielding

$$\kappa = \frac{K_z}{K_d + K_z} = \frac{7.35}{28.65} = 0.26$$

It is noted that κ values for other conditions could also have been derived, which however would have made a reevaluation of the existing plate sinkage tests mandatory in terms of equation 18 with $n = 0.833$. In the framework of this exploratory study, this was not deemed necessary.

Pull/load ratio on air-dry sand

51. Test 11[6] yielded a pull/load ratio of 0.465 (table 4, reference 6) for an average friction angle (shear plate) of $\phi = 30$ deg (table 1, reference 6, S_1 condition) and cohesion $c = 0$. With these values, equation 35 yields a pull/load ratio of

$$\frac{P}{W} = (1 - 0.026)(1 - 0.13) \cos 5.2 \text{ deg} \tan 30 \text{ deg} = 0.487$$

which is less than 5 percent off the measured value of 0.465.

Pull/load ratio on wet sand

52. To simulate the small amount of cohesion exhibited by the lunar surface, the sand was wetted so as to obtain a certain amount of apparent cohesion.[6] For one test (No. 49 in table 2 of reference 6), the exponent of the pressure-sinkage relation was 0.79, which is close enough to the required value of 0.833. The corresponding k_c and k_ϕ values were 5.42 lb/in.$^{1+n}$ and 13.38 lb/in.$^{2+n}$, respectively. Since these values refer to the formula $\sigma = \left(k_\phi + \frac{k_c}{b}\right) z^n$ where b is the width of the test plate, the k value as used in this report is (equations 18 and 20)

$$k = 13.38 + \frac{5.42}{10} = 13.92 \text{ lb/in.}^{2+n} = 62 \text{ N/in.}^{(3m+2)/2m}$$

where the 10 in the denominator is the wheel width (in inches).

53. Unfortunately, test 49, for which these values were derived, was not made with a Bendix wheel. On the other hand, these numerical values refer to the C_2 soil condition, on which various Bendix wheel

first-pass tests were made with loads varying from 67 to 670 N. Therefore, the above-mentioned k value can be used for the evaluation of equation 35 against the results of tests 32 and 86 (table 4, reference 6), which represent these two extreme loads for the C_2 soil condition. The apparent cohesion for this condition was (paragraph 68, reference 6) 0.1 kN/m^2 = 0.0646 $N/in.^2$, and the angle of internal friction as determined with the shear plate was 31.3 deg (table 1, reference 6). The κ value is determined as described in paragraph 50.

$$K_d = 21.3 \ (in.^2 \ N^{-m/2})$$

$$K_z = \frac{126.4^{5/8}}{62^{3/8}} = 4.38 \ (in.^2 \ N^{-m/2})$$

yielding

$$\kappa = \frac{K_z}{K_d + K_z} = 0.17$$

This low value of 0.17, as compared with the previously obtained value of 0.26 (paragraph 50), reflects the higher soil strength of the C_2 condition.

54. Heavy-load test. Test 32 in table 4 of reference 6 yielded a pull/load ratio of 0.529 for the Bendix wheel under a 670-N load. With

$$\sigma = \frac{W^{5/8}}{K_d + K_z} = \frac{670^{5/8}}{25.68} = 2.27 \ N/in.^2$$

$$r_c = 1 - 0.1\kappa = 1 - 0.017 = 0.983$$

$$r_s = 1 - 0.5\kappa = 1 - 0.085 = 0.915$$

$$r_n = 1 - 0.5\kappa \frac{\sqrt{c\sigma \tan \phi}}{c + \sigma \tan \phi} = 1 - 0.085 \frac{\sqrt{0.0894}}{0.0646 + 1.38} = 0.983$$

$$\theta_f' = 3.4 \text{ deg}$$

$$\theta_c' = 3.1 \text{ deg}$$

equation 35 yields

$$\frac{P}{W} = 0.983 \cdot 0.915 \cdot 0.983 \left(0.608 \cdot 0.998 + 25.68 \cdot 0.0646 \sqrt{0.0002934 \cdot 0.999}\right) = 0.884 \ (0.6065 + 0.0285) = 0.56$$

which is about 6 percent off the measured value of 0.529.

55. Light-load test. Test 86 in table 4 of reference 6 yielded a pull/load ratio of 0.664 under the extremely light load of 67 N. Besides the load, only σ, and thus r_n, changes slightly in comparison with the previous case. With $\sigma = 0.539$ N/in.^{2}, equation 35 yields

$$\frac{P}{W} = 0.983 \cdot 0.915 \cdot 0.968 \left(0.608 \cdot 0.998 + 25.68 \cdot 0.0646 \sqrt{0.00522 \cdot 0.999}\right) = 0.870 \ (0.6065 + 0.120) = 0.633$$

which is less than 5 percent off the measured value.*

Summary

56. It thus appears that the semiempirical formula predicts fairly well the P/W ratio of highly flexible elastic-rim wheels on soils with little or no cohesion. Since the equation used (equation 35) is a special version of the pull equation (equation 34), this conclusion is felt to be valid also with respect to equation 34, for which no numerical check is possible because of the lack of test data. On the other hand, it is recognized that the small number of only three numerical validations out of a wealth of available test data might not be considered sufficient to prove the validity of these equations. However, these tests were not selected with a biased viewpoint, but exclusively with regard to the requirement of $n = 0.833$ (paragraph 49), which is based on $m = \bar{m} = 0.75$. Further

---

* Test 83 in table 4 of reference 6 on a slightly stronger soil, but under otherwise identical conditions, yielded $P/W = 0.754$, a debatable result that stands out in a rather isolated manner. No other wheel test of the entire lunar trafficability program yielded a P/W ratio of more than 0.700.

investigations are necessary to determine how much n can deviate from the required value (as constrained by the value of m and the requirement that $m = \bar{m}$) and still result in reliable predictions of pull and slope-climbing capability by equations 34 and 35.

PART IV: MODIFICATION OF EQUATIONS TO INCLUDE RIGID-WHEEL PERFORMANCE

Immobilization Load

57. As the deformability of the wheel decreases and that of the soil increases, the wheel performance in terms of pull/load ratio and slope-climbing capability depends more and more on load W. In the extreme case of rigid wheels on yielding soils, there always exists a limiting load W_i that completely immobilizes the wheel, as illustrated in fig. 9 (from reference 7) and fig. 10. Fig. 9 shows W_i for 28-in.-diam wheels in air-dry Yuma sand (40-45 cone index*) to be 1360 lb (6000 N) for the 12-in.-wide wheel and 680 lb (3000 N) for the 6-in.-wide wheel; W_i for the 3-in.-wide wheel could not be determined from this figure. The same information is presented in fig. 10 (computed from the original test data in table 1 of reference 7) and shows the P/W ratio for these rigid wheels as a function of the load/immobilization load ratio W/W_i. The wheel performance in terms of P/W ratio increases steadily with decreasing W and reaches its theoretical maximum for the hypothetical zero load condition.

58. Equations 34 and 35 were derived by extrapolation from the results on an unyielding surface for which the soil-induced immobilization is irrelevant. Consequently, these equations do not show any dependency of wheel performance on W for purely frictional surface materials, as indicated by the horizontal line in fig. 10. Therefore, these equations necessarily fail in the range of high κ values and need to be modified by additional corrective terms. The nature of the correction must be such that, on one hand, the variation pattern for rigid wheels as shown in fig. 10 is approximated, and on the other hand, that the load effect diminishes rapidly as relative wheel flexibility increases. In other words, the correction must be such that the final equation covers in an adequate manner the area between the upper and lower curves in fig. 10, which in turn

---

* This corresponds[8] to a very dense sand (cone penetration resistance gradient G of 3.6-4.05 MN/m3), for which $\phi = 40$ deg (at least) can be assumed.

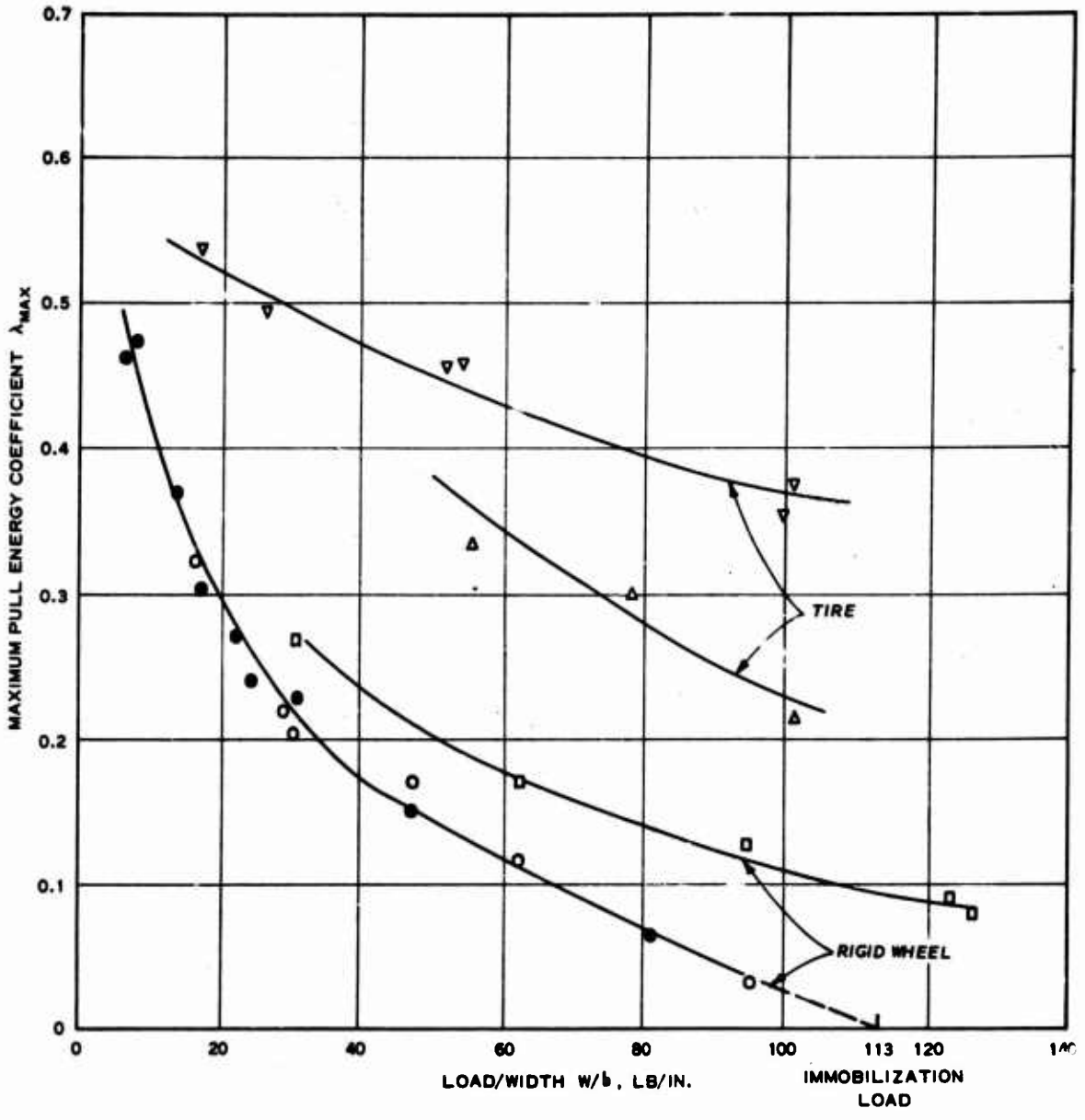

Fig. 9. Variation of P/W ratio with axle load for various wheels on sand (adapted from reference 7)

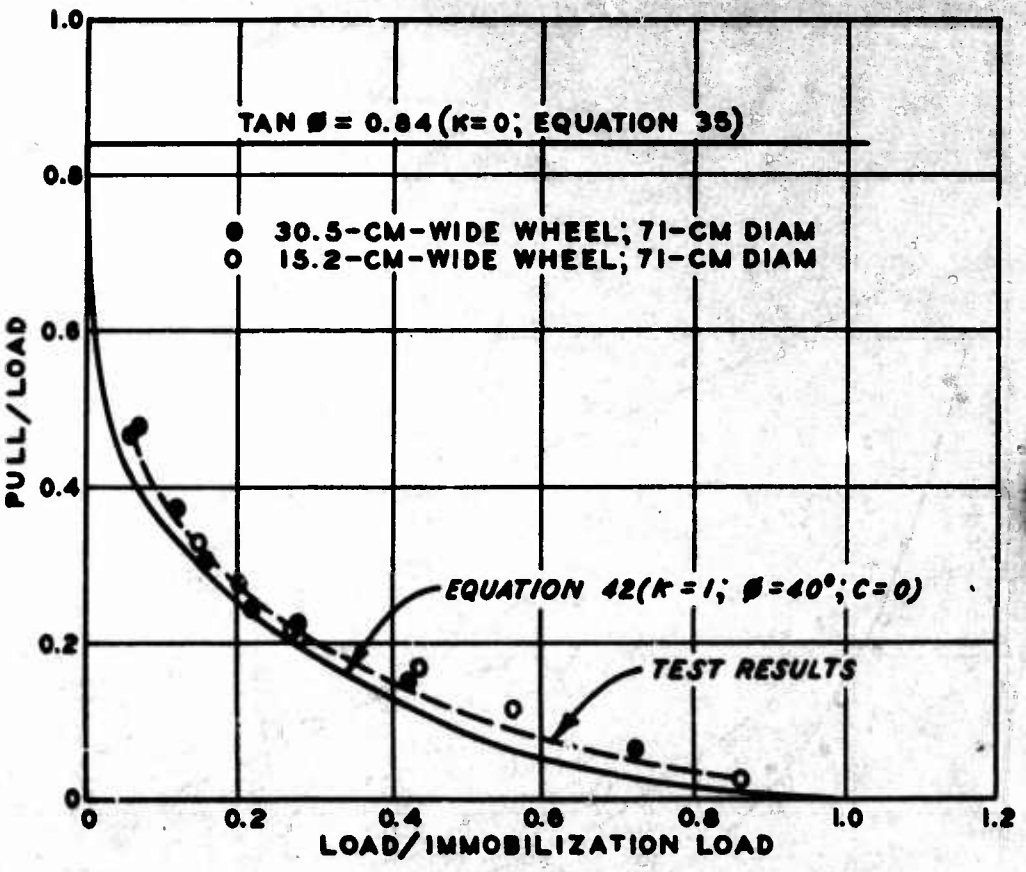

Fig. 10. P/W versus W/W_i for rigid wheels on sand. Data points computed from table 1, reference 7

represent the fix points $K = 0$ and $K = 1$ for a frictional surface material of a given shear strength.* At the same time, the modified equation must satisfy these fix points rigorously so as to securely anchor the extrapolation at both sides of the K spectrum.

Modification of Reduction Factors

59. Experimentation with various mathematical expressions showed that modification of the reduction factors to fit rigid-wheel performance

---

* Similar test results with rigid wheels on purely cohesive material are not available. It will, therefore, be assumed, in the framework of this study, which focuses on lunar soils with only a small amount of cohesion, that the correction applies likewise to the frictional and the cohesive terms of the equations.

can be achieved by a two-step procedure. First, a fourth reduction term of the form

$$r_i = \left(1 - \kappa \frac{W}{W_i}\right)^2 \tag{36}$$

is added to equations 34 and 35, where W_i is the immobilization load of the corresponding rigid-wheel version of the wheel considered on level ground.* The reduction factor is quadratic to express in the simplest possible fashion the nonlinearity of the lower curve of fig. 10.

60. While this addition of equation 36 to equations 34 and 35 correctly yields zero P/W ratio for $W = W_i$, it does not account for the theoretical maximum $P/W = \tan \phi$ for $W/W_i = 0$, which holds true even for rigid wheels, as indicated by fig. 10. To satisfy this condition, the negative terms in the correction factors r_c, r_s, and r_n (paragraph 43) must be modified so as to vanish for $W/W_i = 0$, but without being reduced too much in intermediate conditions. This can be achieved by associating each of these terms with a factor of the form $\left(W/W_i\right)^{n'}$, which has the required properties of $n' \ll 1$. Experimentation with various numbers showed $n' = 1/12$ to be satisfactory. The following modified reduction factors are therefore proposed:

$$r_c' = 1 - 0.1\kappa \left(\frac{W}{W_i}\right)^{1/12} \tag{37}$$

$$r_s' = 1 - 0.5\kappa \left(\frac{W}{W_i}\right)^{1/12} \cos \theta \tag{38}$$

$$r_n' = 1 - 0.5\kappa \left(\frac{W}{W_i}\right)^{1/12} \frac{\sqrt{c\sigma \tan \phi}}{c + \sigma \tan \phi} \cos \theta \tag{39}$$

to which the fourth factor

$$r_i = \left(1 - \kappa \frac{W}{W_i}\right)^2 \text{ (equation 36)}$$

is added to the general formulation of equations 34 and 35.

---

* The cosine term to account for the normal load components on slopes cancels out in the ratio W/W_i.

61. It appears logical at this point to include the additional slope angles θ_f' and θ_c' in this reasoning and to make them, too, dependent on the W/W_i ratio. While these angles probably are relatively independent of sinkage (i.e. load) under normal conditions (paragraph 31), it is nevertheless obvious that these angles are zero for zero load and maximum for the immobilization load. A nonlinear variation of the θ' angles with the W/W_i ratio is proposed, and the definitions of θ_f' and θ_c' (paragraphs 29-34) are modified as follows:

$$\theta_f' = \theta_c' = \theta' = \kappa \left(1 + 0.25 \frac{\theta}{\phi}\right)\left(\frac{W}{W_i}\right)^{1/2} \theta_i' \qquad (40)$$

where θ_i' is the angle as determined for the corresponding rigid wheel under immobilization load on level ground, and the exponent $1/2$ has been arbitrarily chosen to express the nonlinearity of the relation. For the purpose of this study, θ_i' will be assumed to be 40 deg.

Modified Version of Final Equation

62. With these reduction factors, the final pull equation is presented in unabridged form for reference purposes:

$$P = \left[1 - 0.1\kappa \left(\frac{W}{W_i}\right)^{1/12}\right]\left[1 - 0.5\kappa\left(\frac{W}{W_i}\right)^{1/12} \cos\theta\right]$$
$$\times \left[1 - 0.5\kappa\left(\frac{W}{W_i}\right)^{1/12} \frac{\sqrt{c\sigma \tan\phi}}{c + \sigma \tan\phi} \cos\theta\right]\left(1 - \kappa \frac{W}{W_i}\right)^2$$
$$\times \left[W \cos(\theta + \theta') \tan\phi + (K_z + K_d)\, c\sqrt{W^m \cos^m(\theta + \theta')}\right] - W \sin\theta \qquad (41)$$

from which the P/W ratio on level ground is derived by making $\theta = 0$:

$$\frac{P}{W} = \left[1 - 0.1\kappa\left(\frac{W}{W_i}\right)^{1/12}\right]\left[1 - 0.5\kappa\left(\frac{W}{W_i}\right)^{1/12}\right]\left[1 - 0.5\kappa\left(\frac{W}{W_i}\right)^{1/12} \frac{\sqrt{c\sigma \tan\phi}}{c + \sigma \tan\phi}\right]$$
$$\times \left(1 - \kappa \frac{W}{W_i}\right)^2 \left[\cos\theta' \tan\phi + (K_z + K_d)\, c\sqrt{W^{m-2} \cos^m \theta'}\right] \qquad (42)$$

The slope-climbing capability is obtained in the implicit form by making $P = 0$. Although equations 41 and 42 were developed to cover the range of high κ values, particularly $\kappa = 1$, the numerical check against the available test results shows them to be appropriate also in the range of low κ values, including $\kappa = 0$* . Therefore, these equations can be considered the first definite result of the semiempirical approach.

Numerical Verification

Rigid wheel on level sand

63. For $\kappa = 1$ and $c = \theta = 0$, equation 42 yields

$$\frac{P}{W} = \left[1 - 0.1\left(\frac{W}{W_i}\right)^{1/12}\right]\left[1 - 0.5\left(\frac{W}{W_i}\right)^{1/12}\right]\left(1 - \frac{W}{W_i}\right)^2 \cos\theta' \tan\phi$$

With $\theta' = \left(\frac{W}{W_i}\right)^{1/2} \cdot 40$ deg (equation 40) and an assumed value of $\phi = 40$ deg, equation 42 yields the P/W ratio as a function of the W/W_i ratio, which is plotted in fig. 10. The general trend of this curve, as well as the numerical values, agrees remarkably well with the test data indicating that the chosen corrective terms are appropriate for the rigid-wheel condition.

Bendix wheel

64. To show that the modified final equation (equation 42) does not yield significantly different results from those from the first version (equation 35) in the range of highly flexible wheels, the numerical evaluation of the investigated cases (paragraphs 48-56) is repeated on the basis of equation 42 with the same input values as those previously used.

65. Pull/load ratio on air-dry sand (test 11, reference 6). The previously used numerical values were (paragraphs 48-51): $\theta = 0$, $c = 0$, $\phi = 30$ deg, and $\kappa = 0.26$. The modified equation requires, in addition, the knowledge of W and W_i of the corresponding rigid wheel (R = 20 in., B = 10 in.). From table 4, reference 6, W is 310 N, and W_i is estimated to be 7000 N, which is somewhat higher than that measured for the

---

* Only equation 42 was checked numerically (paragraph 48).

smaller rigid wheel (R = 14 in., B = 12 in.) used in reference 7. Finally, angle θ from equation 40 is

$$\theta' = 0.26 \left(\frac{310}{7000}\right)^{1/2} \cdot 40 \text{ deg} = 2.2 \text{ deg}$$

With these values, equation 42 yields

$$\frac{P}{W} = \left[1 - (0.1 \cdot 0.26 \cdot 0.77)\right]\left[1 - (0.5 \cdot 0.26 \cdot 0.77)\right]\left[1 - (0.26 \cdot 0.044)\right]^2$$

$$\times \cos 2.2 \text{ deg} \tan 30 \text{ deg} = 0.98 \cdot 0.90 \cdot 0.975 \cdot 0.998 \cdot 0.578 = 0.495$$

The previously obtained value (paragraph 51) was $P/W = 0.487$.

66. Pull/load ratio on wet sand (test 32, reference 6). The previously used numerical values were (paragraphs 52-55): $\theta = 0$; $c = 0.0646$ N/in.^{2} ; $\phi = 31.3$ deg ; $\kappa = 0.17$; $K_d + K_z = 25.68$ (in.^{2} N$^{-m/2}$) ; $W = 670$ N ; $m = 0.75$; and $\sigma = 2.27$ N/in.^{2} Once more W_i is estimated to be 7000 N, and θ from equation 40 is 2.1 deg. With these values:

$$r_c' = 1 - (0.1 \cdot 0.17 \cdot 0.82) = 0.986 \text{ (equation 37)}$$

$$r_s' = 1 - (0.5 \cdot 0.17 \cdot 0.82) = 0.930 \text{ (equation 38)}$$

$$r_n' = 1 - (0.5 \cdot 0.17 \cdot 0.82 \cdot 0.207) = 0.986 \text{ (equation 39)}$$

$$r_i' = \left[1 - (0.17 \cdot 0.0956)\right]^2 = 0.968 \text{ (equation 36)}$$

And equation 42 yields

$$\frac{P}{W} = 0.986 \cdot 0.930 \cdot 0.986 \cdot 0.968 \left[\cos 2.1 \text{ deg} \tan 31.3 \text{ deg} + (25.68\right.$$

$$\left. \cdot 0.0646 \cdot 670^{-5/8} \cos^{3/8} 2.1 \text{ deg})\right] = 0.875 (0.607 + 0.0285) = 0.556$$

The previously obtained value (paragraph 54) was $P/W = 0.56$.

67. For the light-load test (paragraph 55), the influence of the W/W_i term is obviously negligible, so that a reevaluation of this test can be omitted. For the hypothetical case $W = 0$, equation 42 assumes the same form as that for $\kappa = 0$, indicating that both conditions are identical.

This result is correct, since in both cases the theoretical maximum performance is obtained. This is illustrated in fig. 11, which is a generalization of fig. 10 for frictional material. The $W = 0$ condition is represented by

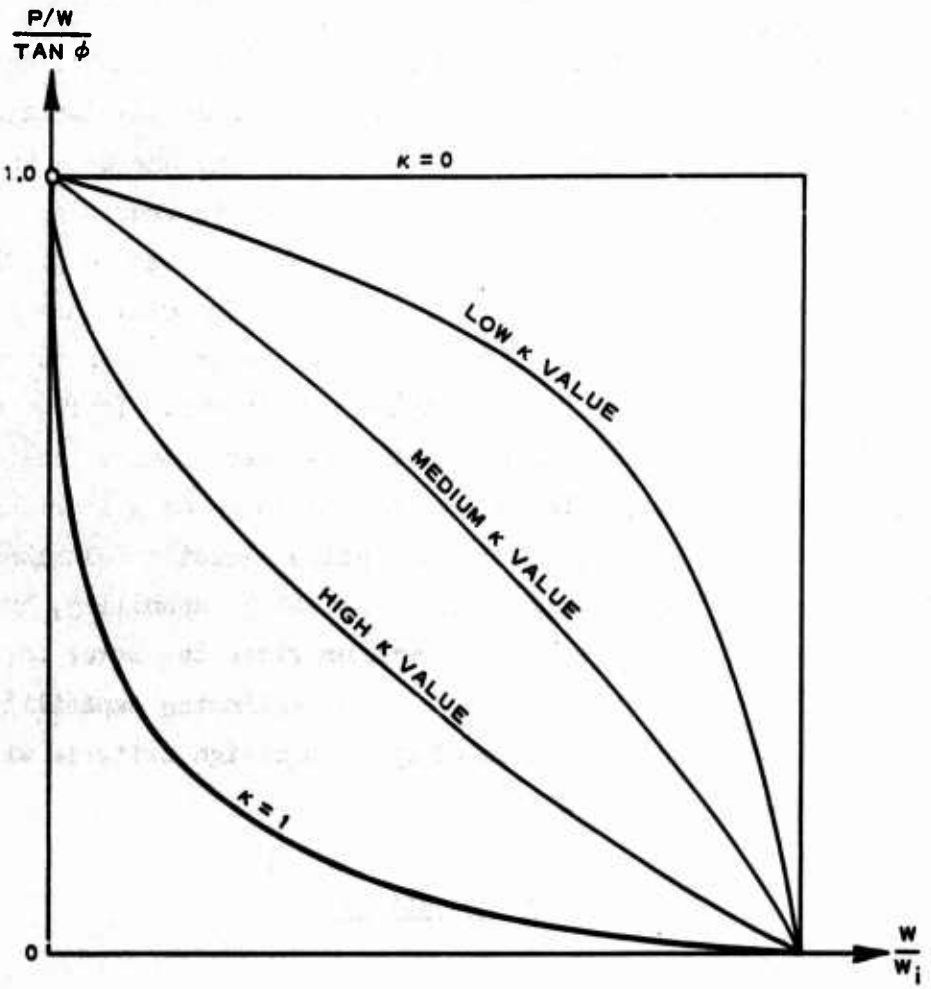

Fig. 11. Schema of performance relations for wheels on level frictional soil

a point, and the $\kappa = 0$ condition by the horizontal line of maximum $P/W = \tan \phi$. The rigid-wheel condition ($\kappa = 1$) is schematically indicated by the lower curve, and some intermediate cases are also given. In fact, fig. 11 is another illustration of the extrapolation process carried out in this study. Equation 35 represents the extrapolation starting from the $\kappa = 0$ line, and equation 42, the extrapolation starting from the $\kappa = 1$ line. The numerical verification for the intermediate conditions $\kappa = 0.17$ and $\kappa = 0.26$ shows that both extrapolations "meet" each other neatly, at least for the level-ground condition.

PART V: CONCLUSIONS AND RECOMMENDATIONS

Conclusions

68. The present study is a beginning. Its intent was to demonstrate that besides a purely empirical approach (which necessarily lacks generality) and a purely theoretical approach (which so far has been unsuccessful), a semiempirical approach to wheel performance is feasible. The principal result of this effort is equation 41, which was used to predict wheel performance in terms of the pull/load ratio for the special case of level ground (equation 42). This prediction was satisfactory, both quantitatively and qualitatively, for a wide range of wheel conditions. It is, therefore, concluded that a semiempirical approach to wheel performance prediction is feasible and that equation 41 is well suited to serve as a starting point.

69. The scope of this study did not allow direct conclusions to be drawn with respect to the problem of slope-climbing capability, but it is believed that the approach developed herein provides the means for developing a numerical prediction system for the slope-climbing capability of single wheels and the identification of optimum design criteria with regard to slope-climbing capability.

Recommendations

70. It is, therefore, recommended that:

a. A computer study be conducted to determine the numerical value of $\lambda = \frac{\tan \theta}{(P/W)_Q}$ as a function of the parameters in equation 41. Since both the numerator and the denominator of this ratio represent special cases of the same equation (equation 41), the uncertainties resulting from the various assumptions can be expected to cancel out so that the numerical values of λ represent a reliable link between the P/W ratio on level ground and the slope-climbing capability.

b. A few check tests be conducted in those regions of the K spectrum and the soil spectrum that have not yet been

explored (i.e. $K = 0.4\text{-}0.8$, true $c\text{-}\phi$ soil, and purely cohesive soil) and to modify equation 41 accordingly, if necessary.

c. Modifying coefficients that will permit inclusion of pneumatic tires in the system be developed and checked.

LITERATURE CITED

1. Hansen, J. B., "Discussion of Hyperbolic Stress-Strain Response: Cohesive Soils," Journal, Soil Mechanics and Foundation Division, American Society of Civil Engineers, Vol 89, No. SM4, July 1963, pp 241-242.

2. Murphy, N. R., Jr., "Measuring Soil Properties in Vehicle Mobility Research; An Evaluation of the Rectangular Hyperbola for Describing the Load-Deformation Response of Soils," Technical Report No. 3-652, Report 2, Oct 1965, U. S. Army Engineer Waterways Experiment Station, CE, Vicksburg, Miss.

3. Green, A. J. and Murphy, N. R., Jr., "Stresses Under Moving Vehicles; Distribution of Stresses Beneath a Towed Pneumatic Tire in Air-Dry Sand," Technical Report No. 3-545, Report 5, July 1965, U. S. Army Engineer Waterways Experiment Station, CE, Vicksburg, Miss.

4. Wiendieck, K. W., "Contribution to the Mechanics of Rigid Wheels on Sand," Technical Report M-68-2, May 1968, U. S. Army Engineer Waterways Experiment Station, CE, Vicksburg, Miss.

5. _____, "Stress-Displacement Relations and Terrain-Vehicle Mechanics: A Critical Discussion," Journal of Terramechanics, Vol 5, No. 3, 1968, pp 67-85.

6. Freitag, D. R., Green, A. J., and Melzer, K.-J., "Performance Evaluation of Wheels for Lunar Vehicles," Technical Report M-70-2, Mar 1970, U. S. Army Engineer Waterways Experiment Station, CE, Vicksburg, Miss.

7. Leflaive, E. M., "Mechanics of Wheels on Soft Soils; Effect of Width on Rigid Wheel Performance," Technical Report No. 3-729, Report 2, Nov 1967, U. S. Army Engineer Waterways Experiment Station, CE, Vicksburg, Miss.

8. Melzer, K.-J., "Measuring Soil Properties in Vehicle Mobility Research; Relative Density and Cone Penetration Resistance," Technical Report No. 3-652, Report 4, July 1971, U. S. Army Engineer Waterways Experiment Station, CE, Vicksburg, Miss.